GEOPHYSICAL RESEARCH LETTERS, VOL. 27, NO. 10, PAGES 1519-1522, MAY 15, 2000

The impact of rising atmospheric CO_2 on simulated sea ice induced thermohaline circulation variability

Marika M. Holland[1], Aaron J. Brasket, Andrew J. Weaver

University of Victoria, Victoria, B.C., Canada

Abstract. The impact of rising atmospheric CO_2 levels on the sea ice induced low frequency variability of the North Atlantic climate is examined using a coupled ice/ocean/atmosphere model. In particular, we focus on thermohaline circulation variability forced by fluctuations in ice export from the Arctic basin. Under $2XCO_2$ conditions, the thermohaline circulation variance is reduced to 7% of its simulated value under present day forcing. This decrease is caused by relatively low ice export variability and changes in the primary ice melt location in the northern North Atlantic under $2XCO_2$ conditions.

Introduction

Observations show that the North Atlantic climate system possesses pronounced interdecadal variability in its sea ice, ocean and atmosphere components [Deser and Blackmon(1993)]. The long timescale associated with this variability suggests that the ocean, and in particular the thermohaline component, may play an integral role in its mechanism.

Sea-ice export from the Arctic Ocean is an important source of fresh water for the North Atlantic. This export is highly variable [Kwok and Rothrock(1999)] and has the potential to force variability in the North Atlantic system. The presence of sea ice also impacts the heat budget through its insulation of the ocean from the relatively cold overlying atmosphere. Modeling studies [Mauritzen and Häkkinen(1997)] have shown that variations in Arctic ice export influence the North Atlantic deep water formation rates.

Sea ice effects also play an important role in the climate response to rising atmospheric CO_2 levels. Recent evidence [Vinnikov et al.(1999)] suggests that the Arctic sea ice extent is decreasing due to anthropogenic climate change. Observed and possible future changes in the ice cover will modify high latitude ocean-atmosphere characteristics and exchange.

A question which naturally arises concerns how sea ice induced North Atlantic climate variability will change under increased atmospheric CO_2 levels. Modeling studies [Gordon and Hunt(1994)] have examined the effect of increased atmospheric CO_2 on atmospheric variability using fairly short (20-80 year) integrations.

Here we use a coupled ice/ocean/atmosphere model in an attempt to quantify potential changes in North Atlantic interdecadal climate variability under increased atmospheric CO_2. We focus our attention on thermohaline circulation (THC) variability induced by fluctuations in Arctic ice export. The simulated variability under present-day and $2\times CO_2$ forcing is compared.

Experimental Design

A global coupled ice/ocean/atmosphere model [Fanning and Weaver(1996)] is used in this study. The model has no flux corrections and is forced with seasonally varying incoming solar radiation and surface wind stress. Improvements have been made to the original model, with particular attention given to high latitudes.

The ocean component of the model is the Geophysical Fluid Dynamic Laboratory Modular Ocean model, version 2 (MOM2) [Pacanowski(1995)]. It has a resolution of 3.6° longitude by 1.8° latitude and 19 vertical levels (varying in depth from 50 m near the surface to approximately 500 m at depth).

The atmospheric component of the model is an energy/moisture balance model (EMBM), with the same horizontal resolution as the ocean component and no atmospheric dynamics. Heat and water vapor transport are parameterized as diffusive processes. Changing atmospheric CO_2 levels are accounted for by applying a radiative forcing perturbation to the outgoing planetary longwave flux. This radiative forcing reaches 4 W m^{-2} at the time of CO_2 doubling. Because of the lack of atmospheric dynamics, wind forcing is specified in the model. This precludes any dynamical atmospheric feedbacks in the model system. However, the relative simplicity of the atmospheric model allows us to run integrations of several thousand years in duration.

A dynamic sea ice formulation [Hunke and Dukowicz (1997)] is included in the current model. This model has a sub-grid scale ice thickness distribution which allows ten ice categories to occur within each model grid cell [Hibler(1980)].

A rotation of the coupled model grid is used to avoid the problem of converging meridians near the north pole, and to better resolve processes within the Arctic Ocean [Eby and Holloway(1994)]. A simple Euler angle rotation displaces the North Pole 13° south into Greenland, while the South Pole remains within Antarctica.

At the resolution used here, the model has little inherent variability. In order to drive variability, daily stochastic forcing is applied to the climatological wind stress over the Arctic/North Atlantic sea ice cover. This forcing has a random timeseries and a spatial pattern which is based on an empirical orthogonal function (EOF) analysis of forty years

[1]Now at National Center for Atmospheric Research, Boulder, Colorado.

Paper number 1999GL010949.
0094-8276/00/1999GL010949$05.00

of daily surface pressure data from NCEP reanalysis. The forcing is applied to the sea ice momentum budget. The surface ocean is not affected by the stochastic forcing as only a climatological stress is applied there. This allows us to isolate the effects of variable ice motion on the climate system and simplifies the interpretation of our results. Apart from the seasonal cycle, any simulated oceanic variability is caused by changes in the ice-induced buoyancy forcing.

A spin-up run with no stochastic forcing is used to initialize a 2500 year long integration which is forced with stochastic wind anomalies. The first 1000 years of the stochastic integration are run with present-day forcing, while the additional 1500 years of integration incorporate increasing atmospheric CO_2. The atmospheric CO_2 increases at 1% per year from year 1000 until year 1070, by which time the atmospheric CO_2 concentration has doubled. The forcing then remains at $2\times CO_2$ levels for the final 1430 years of integration.

Results

The timeseries of the overturning index, defined as the maximum value of the annual average North Atlantic meridional streamfunction, is shown in Figure 1a. This includes the initial 1000 year integration under present day forcing and the following 1500 year integration under increased atmospheric CO_2. Low amplitude variability, with a standard deviation of 1.9 Sv, is present in the overturning index under present day forcing. The size of the simulated THC variability is similar to that in coupled general circulation models [Delworth et al.(1993)], suggesting that sea ice effects may be responsible for driving a considerable fraction of the THC variability in these studies. The THC variability shown here has a generally red spectrum with enhanced power at interdecadal timescales (Figure 1b).

The simulated Arctic ice export (Figure 2a), defined to be the volume of ice transported through Fram Strait plus that transported southward from the Barents Sea, has a mean value of 3100 $km^3\ yr^{-1}$ and a standard deviation of 1200 $km^3\ yr^{-1}$ under present-day forcing. This ice export forces the simulated THC variability. Figure 2b shows a regression of the overturning index on the ice export timeseries and reveals that the two are negatively correlated, with ice export leading the overturning changes by 4-5 years. Low Arctic ice export reduces ice melt in the northern North Atlantic. This destabilizes the water column, leading to enhanced convection the following winter. Warm sea surface anomalies result due to changes in convection and an increase in northward ocean heat transport. This decreases the wintertime ice growth. Idealized modeling studies [Yang and Neelin(1997)] suggest that this leads to a negative feedback with an oscillatory solution. Although the variability obtained here is considerably different from that of Yang and Neelin, we believe that a similar mechanism damps the simulated THC variability.

Low frequency variability is also seen in the Arctic Ocean temperatures and is linked to changes in the THC. A relatively warm Arctic Ocean occurs during high overturning periods due to increased oceanic heat transport into the Arctic basin. This, in addition to the variable wind forcing, affects the simulated Arctic ice volume variability. At high frequencies, the wind driven variability dominates whereas

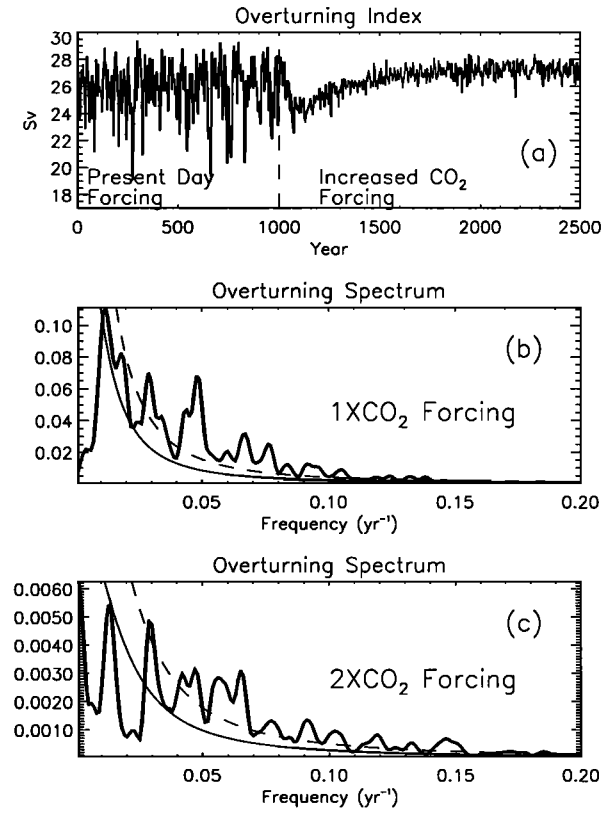

Figure 1. The overturning index a) timeseries, b) spectrum for years 1-1000 and c) spectrum for years 1500-2500. The thin solid line represents the theoretical red spectrum and the dashed line represents the 95% significance level.

at low frequencies ($f < (15\ year)^{-1}$) the wind and heat flux forcing are both important for driving Arctic ice anomalies.

Under rising atmospheric CO_2 levels, the surface air temperatures warm and the ice edge recedes. By the end of the simulation, the annually-averaged global mean air temperature has increased by approximately 3.3 ° C, with the warming amplified at high latitudes. The Atlantic Ocean is also generally warmer under $2\times CO_2$ conditions, with a maximum difference of 6 ° C occurring at the surface of the northern North Atlantic. Although, the North Atlantic undergoes an initial freshening as atmospheric CO_2 increases, its final value after 1500 years of integration is more saline that that of the present day simulation.

The Atlantic layer, which lies between 200 and 800m depth within the Arctic Ocean, is warmer and fresher in the $2\times CO_2$ climate, reaching a maximum anomaly over the Lomonosov Ridge of 0.9 ° C and -0.4 psu. The warming of these waters is reminiscent of recent observations in the Arctic Ocean [Carmack et al.(1995)]. As occurs here, the observed warming appears to be caused by anomalously warm Atlantic waters which penetrate into the Arctic Ocean [Swift et al.(1998)]. The freshening of the Arctic is related to changes in ice melt and transport. Under $2\times CO_2$ forcing, the Arctic ice volume is considerably reduced from 38,000 km^3 to 19,000 km^3.

The THC strength is also affected by the simulated climate change. The overturning undergoes an initial decrease of approximately 0.06 Sv/year during the years of increas-

ing CO_2 (Figure 1a). This results in a maximum decrease of 4.7 Sv, which is qualitatively similar to what has been seen in other studies [Manabe and Stouffer(1994)]. Anomalies of this size are seen throughout the present-day forcing integration, making the initial THC response to rising CO_2 levels difficult to detect against the present-day variability.

Following the initial response to increasing atmospheric CO_2 levels, the overturning recovers, reaching a mean state which is slightly higher than that of the first 1000 years of integration. Using a similar model, Wiebe and Weaver (1999) found a more dramatic increase in the THC strength under $2XCO_2$ forcing. The discrepancy in our results is likely due to different model physics. In particular, sea ice dynamics are absent in the model used by Wiebe and Weaver.

The climate change which occurs under increased CO_2 forcing has a fundamental impact on the simulated THC variability. The overturning variance is greatly reduced (Figure 1a) from 3.6 Sv^2 under present day forcing to 0.25 Sv^2 for the final 1000 years of integration. Under $2XCO_2$ forcing, the variability is still generally concentrated at low frequencies (Figure 1c).

The decrease in THC variability is due to a decrease in the variability of Arctic sea ice export. The mean ice export decreases by approximately 1000 $km^3\ yr^{-1}$ under the $2\times CO_2$ forcing (Figure 2a), and the standard deviation also decreases from 1200 $km^3\ yr^{-1}$ to approximately 720 $km^3\ yr^{-1}$. This decreased variability results from reduced variance in both the ice thickness and ice velocity within the Fram Strait region. Recall that THC variability drives low frequency variability in the Arctic Ocean temperatures, and subsequently the ice growth rates. The reduction of this variability under $2\times CO_2$ conditions results in reduced low-frequency ice thickness variability within the Arctic and is likely responsible for some of the reduction in ice export variability.

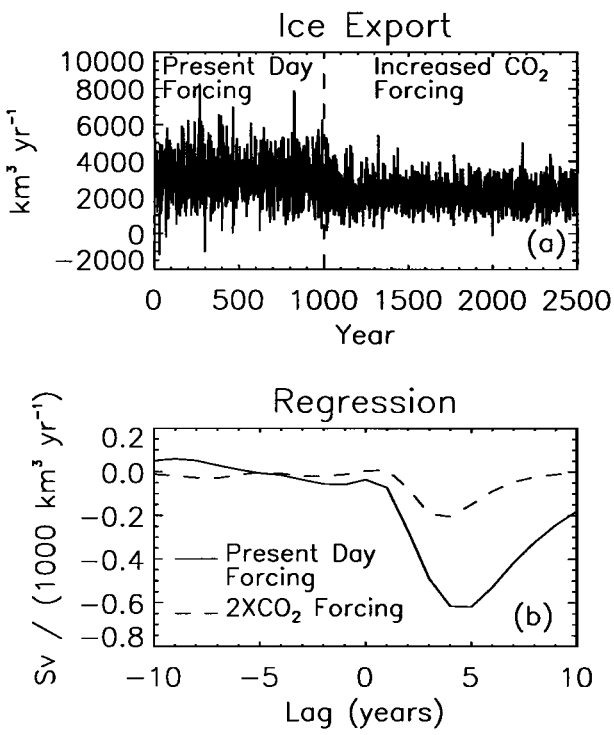

Figure 2. a) The timeseries of Arctic ice export. b) The coefficients of the overturning index regressed on the ice export as a function of lag. A positive lag implies that the export leads changes in the overturning.

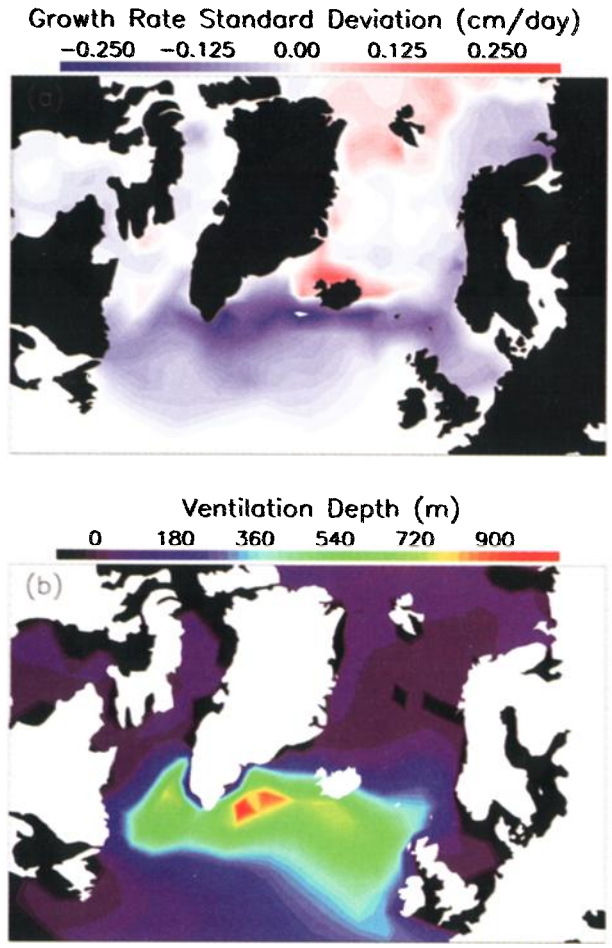

GL10323F03

Figure 3. a) The difference in the ice melt rate standard deviation between the $2\times CO_2$ integration and the $1\times CO_2$ integration. b) The ventilation depths averaged over year 2400-2500 of the integration.

Not only is the ice export variability reduced under $2\times CO_2$ forcing, but it is also less efficient at driving THC changes. This can be seen in the regression of the overturning index on the ice export timeseries (Figure 2b). A 1000 $km^3\ yr^{-1}$ ice export anomaly results in a linear overturning response of 0.6 Sv under $1\times CO_2$ forcing and 0.2 Sv under $2\times CO_2$ forcing. Under $2\times CO_2$ forcing, the primary ice melt location in the North Atlantic shifts northward, resulting in reduced ice melt variability over the simulated convective regions (Figure 3). This reduces the impact of ice export anomalies on convective activity and consequently on the THC variability. Although some of the deep water formation sites (e.g. the Greenland Sea) are not well captured in these simulations (a feature common in many coarse resolution ocean models), this result does point out that changes in the location of ice melt will likely impact the low frequency variability in the North Atlantic.

Conclusions

The results from this study suggest that interactions between sea ice and the thermohaline circulation have the potential to reduce the low-frequency variability in the North Atlantic under climate warming scenarios. Changes in the variability of ice export, the location of ice melt, and the regions of convection all appear to play a role in modifying the simulated variability of the thermohaline circulation. The current study has focused on the often overlooked impacts of sea ice on the variability of the North Atlantic climate and in particular its association with changes in the intensity of the thermohaline circulation. Other interactions of the climate system (e.g. cloud feedbacks, wind stress feedbacks) will also influence the variability of the climate system under rising atmospheric CO_2 levels and the net effect of these various interactions is yet to be determined. Nevertheless, our results suggest the need for the incorporation of more realistic treatments of the Arctic Ocean and its sea ice cover in more complete coupled general circulation models, such as those used to project future changes in climate and climate variability.

Acknowledgment. This research was supported by International Arctic Research Center, NSERC, Atmospheric Environment Service, Canadian Institute for Climate Studies and IBM SUR research grants.

References

Carmack, E. C., R. W. Macdonald, R. G. Perkin, F. A. McLaughlin and R. J. Pearson, 1995: Evidence for warming of Atlantic water in the southern Canadian Basin of the Arctic Ocean: Results from the Larsen-93 expedition. *Geophys. Res. Lett.*, **22**, 1061–1064.

Delworth, T., S. Manabe and R. J. Stouffer, 1993: Interdecadal variations of the thermohaline circulation in a coupled ocean-atmosphere model. *J. Climate*, **6**, 1993–2011.

Deser, C. and M. L. Blackmon, 1993: Surface climate variations over the North Atlantic Ocean during winter: 1900- 1989. *J. Climate*, **6**, 1743–1753.

Eby, M. and G. Holloway, 1994: Grid transformation for incorporating the Arctic in a global ocean model. *Clim. Dyn.*, **10**, 241–247.

Fanning, A. F. and A. J. Weaver, 1996: An atmospheric energy-moisture balance model: Climatology, interpentadal climate change, and coupling to an ocean general circulation model. *J. Geophys. Res.*, **101**, 15111–15128.

Gordon, H. B. and B. G. Hunt, 1994: Climatic variability within an equilibrium greenhouse simulation. *Clim. Dyn.*, **9**, 195–212.

Hibler, W. D., 1980: Modeling a variable thickness ice cover. *Mon. Wea. Rev.*, **108**, 1943–1973.

Hunke, E. C. and J. K. Dukowicz, 1997: An elastic-viscous-plastic model for sea ice dynamics. *J. Phys. Oceanogr.*, **27**, 1849–1867.

Kwok, R. and D. Rothrock, 1999: Variability of Fram Strait ice flux and North Atlantic Oscillation. *J. Geophys. Res.*, **104**, 5177–5189.

Manabe, S. and R. J. Stouffer, 1994: Multiple-century response of a coupled ocean-atmosphere model to an increase of carbon dioxide. *J. Climate*, **7**, 5–23.

Mauritzen, C. and S. Häkkinen, 1997: Influence of sea ice on the thermohaline circulation in the Arctic-North Atlantic Ocean. *Geophys. Res. Lett.*, **24**, 3257–3260.

Pacanowski, R., 1995: *MOM 2 Documentation, user's guide and reference manual. GFDL Ocean Group Tech. Rep. 3.* GFDL, Princeton, NJ.

Swift, J. H., E. P. Jones, K. Aagaard, E. C. Carmack, M. Hingston, R. W. MacDonald, F. A. McLaughlin and R. G. Perkin, 1998: Waters of the Makarov and Canada basins. *Deep Sea Res*, **44**, 1503–1529.

Vinnikov, K. Y., A. Robock, R. J. Stouffer, J. E. Walsh, C. L. Parkinson, D. J. Cavalieri, J. F. B. Mitchell, D. Garrett and V. F. Zakharov, 1999: Global warming and Northern Hemisphere sea ice extent. *Science*, **286**, 1934–1937.

Wiebe, E. C. and A. J. Weaver, 1999: On the sensitivity of global warming experiments to the parameterization of sub-grid scale ocean mixing. *Clim. Dyn.*, submitted.

Yang, J. and J. D. Neelin, 1997: Decadal variability in coupled sea-ice - thermohaline circulation systems. *J. Climate*, **10**, 3059–3076.

M. M. Holland, A. J. Brasket and A. J. Weaver, School of Earth and Ocean Sciences, University of Victoria, P.O. Box 3055, Victoria, BC V8W 3P6, Canada. (e-mail: mholland@ucar.edu)

(Received July 21, 1999; revised February 2, 2000; accepted March 9, 2000.)